2 The Jahn-Teller Effect

Arnout Ceulemans
Department of Chemistry, KU Leuven
Celestijnenlaan 200F, B-3001 Leuven, Belgium

Contents

E. Pavarini and E. Koch (eds.)
Orbital Physics in Correlated Matter
Modeling and Simulation Vol. 13
Forschungszentrum Jülich, 2023, ISBN 978-3-95806-689-2
http://www.cond-mat.de/events/correl23

1 The Jahn-Teller theorem

In 1937 Jahn and Teller wrote:

Theorem 1. *All non-linear nuclear configurations for an orbitally degenerate electronic state are unstable.*

This statement was the beginning of a fruitful line of research both in physics and chemistry. Over the years, it has provided deep theoretical insights as well as important practical applications, in spectroscopy, magnetism, superconductivity and chemical reactivity. First and foremost, the theorem is a particular example of the more general physical principle of *symmetry breaking*. As Pierre Curie once enounced: *c'est la dissymmétrie qui crée le phénomène* (it is the lack of symmetry that creates the phenomenon). The world appears where the initial symmetry is broken, and the phenomena start to abound. This is accompanied by a decrease of temperature, which suggest that the high symmetry state is also highly energetic, and the spontaneous breaking of symmetry is driven by a decrease in energy. In this presentation, the focus will be on the theoretical aspects of the theorem, in particular group theory and topology.[1]

1.1 The distorted rutile structure

At the molecular level degeneracies are usually linked to the presence of symmetry, described by the molecular point groups. A textbook case from structural inorganic chemistry concerns the crystal structures of divalent transition-metal difluorides from CrF_2 to ZnF_2 [2]. These difluorides crystallize according to the rutile structure. Rutile is the mineral of TiO_2. In this structure the metal ions are surrounded by a regular octahedron of six ligands, at equal distances from the central atom. Cr(II) and Cu(II) ions are notable exceptions in the series. For these two metal ions the rutile lattice is distorted, forming a tetragonal coordination, with four equatorial ligands at short distance and two axial ones at longer distances, as indicated in Fig. 1. The figure also shows the crystal field configuration of the d-electrons, with one electron in the e_g shell for Cr(II) and one hole for Cu(II).

The *mean* value of these distances agrees with the expected trends for the d-metal contraction, but clearly some force is distorting the ligand sphere around the ion. What distinguishes these ions form the rest? These are the only two ions in the series for which the ground state configuration is characterized by an odd number of electrons in the e_g shell. The resulting ground states are ${}^2E_g$ multiplets, hence states that are orbitally twofold degenerate. They thus would exemplify the Jahn-Teller (JT) theorem, which states that such ground states are unstable, and will spontaneously distort to lower symmetries. The distortion will lift the degeneracy, and thus remove the cause of instability. Indeed symmetry breaking from O_h to D_{4h} will split the multiplets as follows

$$ {}^2E_g \rightarrow {}^2A_{1g} + {}^2B_{1g}. \tag{1}$$

Further interesting additional observations can also be made:

[1] The presentation, including several figures and formulas, is based on the recent monograph [1].

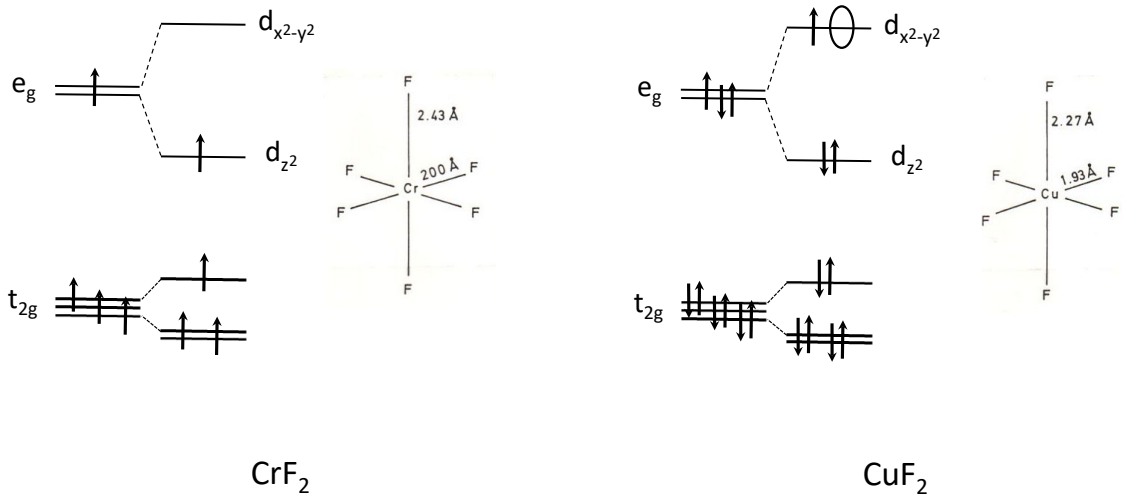

Fig. 1: *Jahn-Teller distortions in CrF_2 and CuF_2*

- The origin of the JT effect is clearly attributed to a local on-site orbital characteristic, which apparently is strong enough to distort the lattice structure. This inscribes the JT theorem in the broad theme of the lecture course.

- It could be argued that similar considerations would apply to the Fe(II) and Co(II) ions which have open t_{2g} shells giving rise to threefold degenerate ground states. These ions are indeed also exemplifying JT instabilities, but the instability is much smaller than in the case of the instabilities caused by the e_g shells. A further distinction is thus in order: the JT force can give rise to molecular structures which are frozen in a particular distorted geometry, or can be weaker and give rise to a vibronic ground state, with dynamic fluctuations. Such fluctuations show up as large anisotropic thermal structure factors in X-ray analysis. We will identify these two regimes as the static versus the dynamic JT effect. In reality however, systems will adopt all sorts of intermediate stages.

- Finally, the symmetry breaking itself is not complete, but rather tries to conserve as much symmetry as possible. Indeed the tetragonal subgroup is the maximal subgroup of O_h, for which d_{z^2} and $d_{x^2-y^2}$ are no longer degenerate. It removes the threefold axes that cause the degeneracy, but keeps all other symmetry elements. This economic principle is known as the epikernel principle.

1.2 Origin of orbital instability

Why is symmetry breaking a spontaneous process in degenerate states? The standard answer to this is that in these states there is always an imbalance between the symmetry of the nuclear charge distribution and the symmetry of the electron density. So electron densities of the individual e_g orbitals have only tetragonal symmetry, while the nuclear distribution is octahedral. The result is a force which acts on the nuclei and displaces them to a new equilibrium position

with D_{4h} symmetry. This argument is based on the fact that for non-degenerate states the electron density always adopts the symmetry of the nuclear frame. For a non-degenerate state $|\Psi\rangle$, a distortion force along a nuclear coordinate Q, is given by

$$F = \frac{\partial}{\partial Q}\langle\Psi|\mathcal{H}|\Psi\rangle|_{Q=0} = \left\langle\Psi\right| \frac{\partial\mathcal{H}}{\partial Q} \left|\Psi\right\rangle\Big|_{Q=0}. \tag{2}$$

If Ψ is non-degenerate, the density $\Psi^*\Psi$, is totally symmetric and the force matrix element can only differ from zero if the Hamiltonian part is likewise totally symmetric, i.e., if the Q-coordinate conserves the symmetry. When extending this argument to degenerate states, it is argued that the average density still is totally symmetric, but that this is no longer true for the density associated with individual components. The sum of the densities of the d_{z^2} and $d_{x^2-y^2}$ states is indeed equal along the three coordinate axes of an octahedron, but the separate densities of the two components is not: it is axial for the d_{z^2} orbital and equatorial for the $d_{x^2-y^2}$ counterpart. In this argument the assumption is made that the electron densities for individual components of degenerate states cannot possibly have the symmetry of the nuclear frame. In fact this is not true. For the twofold degenerate component it suffices to rewrite the components in complex conjugate form, to obtain for both an electron cloud with perfect octahedral symmetry.

$$|\Psi_\pm\rangle = \frac{1}{\sqrt{2}}\left(d_{z^2} \pm i d_{x^2-y^2}\right) \tag{3}$$

Indeed the densities of both these components are equal to the average density of d_{z^2} and $d_{x^-y^2}$, and thus totally symmetric. The real difference between degenerate and non-degenerate states is that in the case of degenerate states, the calculation of the distortion force requires to set up and diagonalize a matrix equation, operating in the degeneracy basis of the state manifold. If for instance we use the $\{\Psi_+, \Psi_-\}$ basis, the JT force will entirely be 'demoted' to the off-diagonal entries of the Hamiltonian matrix.

1.3 The Jahn-Teller Hamiltonian

The potential energy surface in the neighborhood of a JT instability is described by a Taylor series expansion of the Hamiltonian in the coordinate space of active nuclear distortions. The very first and essential terms of the expansion are the first-order force term and the harmonic second-order restoring potential

$$\mathcal{H} = H_0 + \sum_{\Lambda\lambda}\left(\frac{\partial H}{\partial Q_{\Lambda\lambda}}\right)_0 Q_{\Lambda\lambda} + \frac{1}{2}\sum_{\Lambda\lambda} K_\Lambda\, Q^2_{\Lambda\lambda}. \tag{4}$$

Here the distortion Q-coordinates are labeled by an irreducible representation Λ of the high-symmetry molecular point group, and its component or subrepresentation, λ. H_0 is the electronic Hamiltonian in the high-symmetry origin of the coordinate system, relaxed with respect to symmetry-preserving totally symmetric coordinates. Its eigenfunctions are the states of the degenerate manifold. The second-order term is the standard harmonic restoring force, with K_Λ being the harmonic force constant. This term holds the molecular frame together and attracts

the nuclei towards the coordinate origin. The force constant can be obtained from the IR and Raman spectra. The essential term is the linear term, which describes the interaction between the electronic states and the nuclear distortion modes. This linear interaction is the force which pulls the nuclei away from their original symmetry positions. The derivative in this term represents the slope of the energy as a function of the coordinate displacement, evaluated at the high-symmetry point. As a derivative of the Hamiltonian with respect to nuclear positions, this term affects the electron-nuclei Coulomb attraction term, and as a result it is a one-electron operator. This is an important property, which ultimately explains why the JT phenomenon is so tightly linked to orbital properties.

At this point a proper definition of the symmetry properties is in order. The coordinates have already been labeled as $Q_{\Lambda\lambda}$. Likewise the degenerate manifold will be labeled by the degenerate irreducible representation Γ, and its components accordingly by a subrepresentation label γ as $|\Psi^{\Gamma}_{\gamma}\rangle$. The symmetry labels incorporate the entire action of a symmetry element of the point group, $\hat{R} \in G$, on these quantities:

$$\hat{R}Q_{\Lambda\lambda} = \sum_{\lambda'} D^{\Lambda}_{\lambda'\lambda}(R)\, Q_{\Lambda\lambda'} \quad \text{and} \quad \hat{R}|\Psi^{\Gamma}_{\gamma}\rangle = \sum_{\gamma'} D^{\Gamma}_{\gamma'\gamma}(R)\, |\Psi^{\Gamma}_{\gamma'}\rangle. \tag{5}$$

Here the D-matrix elements refer to the irreducible representation (irrep) matrices $\mathbb{D}(R)$ which describe the transformation of the basis functions under all the elements of the symmetry group. What makes the JT Hamiltonian tractable, and in fact extremely attractive, is that instead of working in the entire Hilbert space, it operates in an extremely confined space, comprising at first only the degenerate manifold. Matrix elements of the linear interaction term in this manifold may be factorized according to the Wigner-Eckart theorem as a reduced force element, denoted by the constant F_{Λ}, and a Clebsch-Gordan coupling coefficient, which contains the entire group-theoretical knowledge of the interaction

$$\left\langle \Psi^{\Gamma}_{\gamma_a} \left| \left(\frac{\partial H}{\partial Q_{\Lambda\lambda}} \right)_0 \right| \Psi^{\Gamma}_{\gamma_b} \right\rangle = F_{\Lambda} \left\langle \Gamma\gamma_a | \Lambda\lambda\Gamma\gamma_b \right\rangle. \tag{6}$$

In the second-quantization formalism, we now introduce creation and annihilation operators for the electronic states. Since these are fermionic in nature we label them respectively as $f^{\dagger}$ and f. A normalized N-electron determinant is obtained as a sequence of particles being created from the vacuum state

$$f^{\dagger}_{\alpha} f^{\dagger}_{\beta} ... f^{\dagger}_{\nu} \left|0\right\rangle \equiv \left|\alpha\beta...\nu\right|. \tag{7}$$

The adjoint of this expression is then

$$\left\langle 0\right| f_{\nu} ... f_{\beta} f_{\alpha} = \overline{\left|\alpha\beta...\nu\right|}. \tag{8}$$

Since the linear part of the Hamiltonian involves a one-electron operator, we can express the coupling in operator form as

$$\left(\frac{\partial H}{\partial Q_{\Lambda\lambda}} \right)_0 = \sum_{\gamma_a\gamma_b} f^{\dagger}_{\gamma_a} \left\langle \Psi^{\Gamma}_{\gamma_a} \left| \left(\frac{\partial H}{\partial Q_{\Lambda\lambda}} \right)_0 \right| \Psi^{\Gamma}_{\gamma_b} \right\rangle f_{\gamma_b}. \tag{9}$$

An alternative view point of the interaction involves a recoupling, where the fermion parts are first coupled to an excitation operator with symmetry Λ. This recoupling is carried out by transferring the $\Gamma_b\gamma_b$ irrep of the ket part to the bra, and corresponds to a basic symmetry property of the coupling coefficients [1]. One has, apart from an overall Λ-dependent phase factor which can be incorporated into the force-parameter,

$$\langle \Gamma\gamma_a|\Lambda\lambda\Gamma\gamma_b\rangle = \left(\frac{\dim\Gamma}{\dim\Lambda}\right)^{1/2}\langle\Gamma\gamma_a\Gamma\overline{\gamma_b}|\Lambda\lambda\rangle. \tag{10}$$

Note that the symmetry properties of the annihilation operator, $\Gamma\gamma_b$, appear in the coupling operator as the complex conjugate component, in view of the transfer from ket to bra. Then, these results are inserted into the operator expression, yielding

$$\left(\frac{\partial H}{\partial Q_{\Lambda\lambda}}\right)_0 = k_\Lambda \sum_{\gamma_a\gamma_b} f^\dagger_{\gamma_a}\langle\Gamma\gamma_a\Gamma\overline{\gamma_b}|\Lambda\lambda\rangle f_{\gamma_b}, \tag{11}$$

where k_Λ takes over the role of the F_Λ force elements, by incorporating the dimensional factor

$$k_\Lambda = \left(\frac{\dim\Gamma}{\dim\Lambda}\right)^{1/2} F_\Lambda \tag{12}$$

Vice-versa, since this is a summation over all components, one could as well remove the complex conjugate bar from the coupling coefficient and replace the annihilation operator, f_{γ_b} by its time reversed form, which is denoted by the tilde operator as $\tilde{f}_{\gamma_b}$. The tilde indicates that the annihilation operator $\tilde{f}_{\gamma_b}$ transform in exactly the same way as the corresponding creation operator $f^\dagger_{\gamma_b}$, and as the time reversed of the annihilation operator f_{γ_b}. The operator expression then finally becomes

$$H = k_\Lambda \sum_{\gamma_a\gamma_b}\langle\Gamma\gamma_a\Gamma\gamma_b|\Lambda\lambda\rangle f^\dagger_{\gamma_a}\tilde{f}_{\gamma_b} = k_\Lambda\left(\mathbf{f}^\dagger\mathbf{f}\right)^\Lambda_\lambda. \tag{13}$$

The bracket in the final line of this equation symbolizes the coupling of the fermion creation and annihilation operators to the symmetry of the boson. In this formalism the slope parameter is usually represented as k_Λ. In second quantization we now also add the vibrational mode, expressed in boson creation and annihilation operators

$$Q_{\Lambda\lambda} = \frac{1}{\sqrt{2}}\left(b^\dagger_{\Lambda\lambda} + \tilde{b}_{\Lambda\lambda}\right). \tag{14}$$

Again note the tilde over the annihilation operator. Indeed, both creation and annihilation parts must share the $\Lambda\lambda$ symmetry properties of $Q_{\Lambda\lambda}$. In order to combine the fermionic and bosonic parts it must be taken into account that this involves a scalar product over the Λ tensor, as a fermionic variable and an associated bosonic derivative. Since derivatives and variables transform in conjugate ways, one must write

$$\sum_{\Lambda\lambda}\left(\frac{\partial H}{\partial Q_{\Lambda\lambda}}\right)_0 Q_{\Lambda\lambda} = \sum_\Lambda \kappa_\Lambda\left(\mathbf{f}^\dagger\mathbf{f}\right)^\Lambda \odot \left(\mathbf{b}^\dagger{+}\mathbf{b}\right)_\Lambda. \tag{15}$$

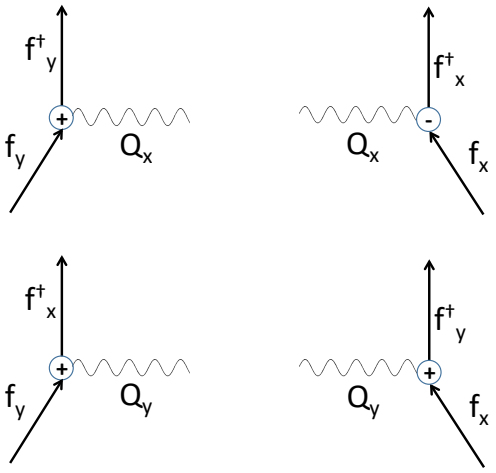

Fig. 2: *Diagram of coupling schemes for the JT matrix elements in the $E \times e$ case (*vide infra*); $f_x^\dagger$ and $f_y^\dagger$ create an electron in resp. d_{z^2} and $d_{x^2-y^2}$ orbitals.*

The dot refers to the scalar product of boson and fermion part which guarantees the total symmetry of the Hamiltonian, due to compensating symmetries in both ingredients. When components follow the spherical (l, m) quantization, the dot product is defined as

$$\left(\mathbf{f}^\dagger\mathbf{f}\right)^l \odot \left(\mathbf{b}^\dagger+\mathbf{b}\right)_l = \sum_m (-1)^m \left(\mathbf{f}^\dagger\mathbf{f}\right)^l_m \left(b^\dagger_{l,-m}+\tilde{b}_{l,-m}\right). \tag{16}$$

The concise second-quantization formalism in Eq. (15) says it all! The fermion creation-annihilation double operator is exactly an excitation operator which requires a field of symmetry $\Lambda\lambda$. This is symbolized for the E-case in Fig. 1.3.
The difference with a proper excitation is that instead of a photon the excitation is brought about by a vibration. To this interaction element one finally adds the harmonic part of the active vibrations. This complements the potential energy of the JT surface with the kinetic energy of the nuclei. The harmonic potential is now replaced by the harmonic oscillator

$$\sum_{\Lambda\lambda} \hbar\omega_\Lambda \Big(b^\dagger_{\Lambda\lambda} b_{\Lambda\lambda} + \frac{1}{2}\Big). \tag{17}$$

The result is a genuine vibronic operator where bosons and fermions meet

$$\mathcal{H} = \sum_\Lambda \kappa_\Lambda \left(\mathbf{f}^\dagger\mathbf{f}\right)^\Lambda \odot \left(\mathbf{b}^\dagger+\mathbf{b}\right)_\Lambda + \sum_{\Lambda\lambda} \hbar\omega_\Lambda \Big(b^\dagger_{\Lambda\lambda} b_{\Lambda\lambda} + \frac{1}{2}\Big). \tag{18}$$

1.4 The pseudo-Jahn-Teller effect

When two electronic states are not strictly degenerate but close together in energy, it should be very surprising that the symmetry breaking mechanism would suddenly be completely quenched. Instead a non-totally symmetric matrix element between both states is symmetry allowed and

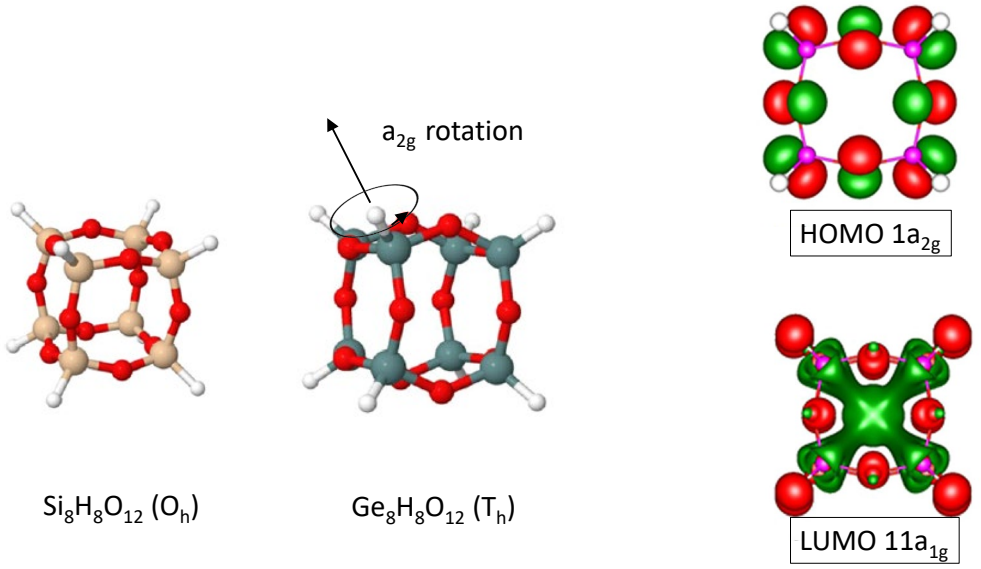

Fig. 3: *Structural comparison between Si and Ge POSS (left), and, HOMO and LUMO for the Ge cluster (right).*

may perfectly well induce a distortion, providing the relaxation term outweighs the harmonic force constant. This is the so-called pseudo-JT effect. Following the formalism of Bersuker [3], let two states be separated by a splitting 2Δ and with an off-diagonal force element FQ, where Q is a non-totally symmetric distortion coordinate. Assume further that the two states share the same force constant K_0. In that case matrix diagonalization leads to the roots

$$E_{\pm} = \frac{1}{2}K_0Q^2 \pm \left(\Delta^2+F^2Q^2\right)^{1/2} = \frac{1}{2}\left(K_0 \pm \frac{F^2}{\Delta}\right)Q^2 \pm \Delta \mp \left(\frac{F^4}{\Delta^3}\right)Q^4 \pm \ldots \qquad (19)$$

If $|\Delta| < F^2/K_0$, then the curvature of the lower energy root becomes negative, and the system will be unstable with respect to Q. An exceptional illustration of this effect is seen in the $O_h \rightarrow T_h$ symmetry breaking in the polyhedral oligomeric sesquioxane (POSS), $Ge_8H_8O_{12}$. While the Silicon isomer has cubic symmetry O_h, it is found by DFT calculations that the Germanium isomer is distorted to the rare tetrahedral symmetry group T_h [4]. In Fig. 3 we display both structures, as well as the HOMO ($1a_{2g}$) and LUMO ($11a_{1g}$) of the Germanium isomer. The off-diagonal matrix element between both orbitals transforms as the direct product: $a_{1g}\times a_{2g} = a_{2g}$. The pseudo-JT effect thus promotes a distortion along the a_{2g} mode. This corresponds precisely to a rotation of the oxygen bridges in between the Germanium atoms. Neighboring vertices on the cube will thereby rotate in opposite directions lowering the symmetry to T_h.

An important caveat is in order here. In principle, for any symmetry breaking it will always be possible to find a pair of interacting states with the right combination of irreducible representations. So the predictive power of the effect is rather limited. A detailed examination of the composition of the relevant orbitals, and a demonstration of the overlap of their off-diagonal density and an observed distortion is required.

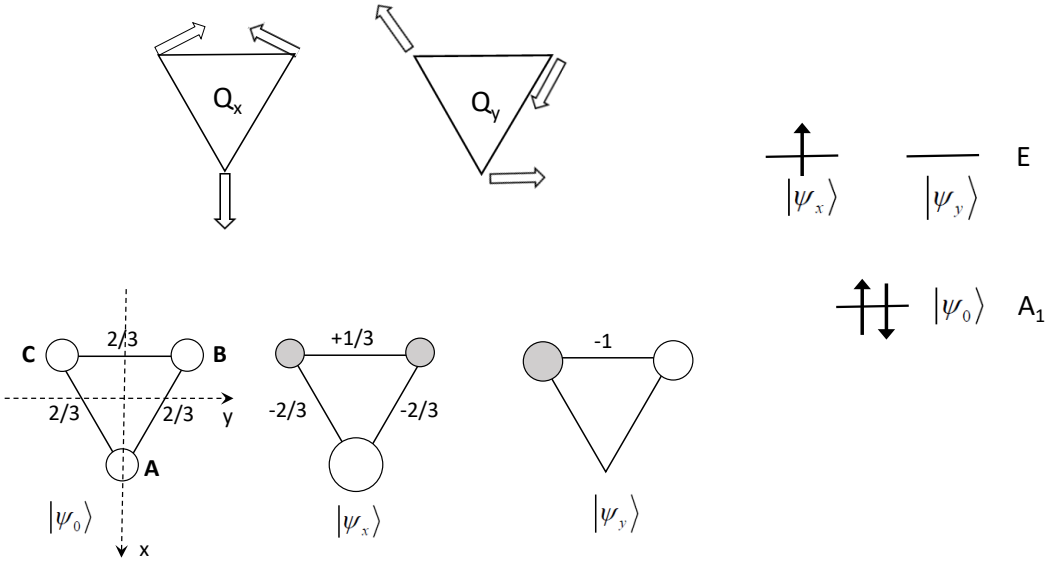

Fig. 4: *Trigonal Na_3 cluster, with doublet ground level; orbitals and distortion modes.*

2 The doublet $E\times e$ Paradigm

The icon of the JT theorem is the Mexican hat potential, corresponding to a twofold degenerate E state, coupled to a twofold degenerate e vibration. This occurs both in cubic and in trigonal or pentagonal symmetry groups. We examine in some detail the standard case of a triangular instability.

2.1 The potential energy surface

The system considered is a tri-atomic molecule in an E state, with components E_x and E_y. The symmetry at the origin is D_{3h}, but since three atoms are coplanar, we could as well work in C_{3v} symmetry. The components are represented schematically in Fig. 4. Their symmetry behavior under the generators of C_{3v} (with right-handed threefold axis) are given by

$$\begin{aligned}
\hat{C}_3 \begin{pmatrix} |Ex\rangle & |Ey\rangle \end{pmatrix} &= \begin{pmatrix} |Ex\rangle & |Ey\rangle \end{pmatrix} \begin{pmatrix} -1/2 & -\sqrt{3}/2 \\ \sqrt{3}/2 & -1/2 \end{pmatrix} \\
\hat{\sigma}_x \begin{pmatrix} |Ex\rangle & |Ey\rangle \end{pmatrix} &= \begin{pmatrix} |Ex\rangle & |Ey\rangle \end{pmatrix} \begin{pmatrix} 1 & 0 \\ 0 & -1 \end{pmatrix}. \qquad (20)
\end{aligned}$$

Here an active view of symmetry operations is adopted: they displace the functions itself, be it orbitals or distortions, while leaving the nuclei in place.
The direct product of the orbital state reads

$$E \times E = \left[a_1{+}e\right] + a_2. \qquad (21)$$

According to the JT selection rule the activity resides in the non-totally symmetric part of the symmetrized product, $[a_1{+}e]$, being the e-vibration. The components of this vibration are also

shown in the figure. They are labeled as Q_x and Q_y. Using local (x, y) coordinates for the individual atoms, the expressions for these vibrations are given by:

$$\begin{aligned} Q_x &= \frac{1}{\sqrt{3}}\left[Q_A^x + \left(-\frac{\sqrt{3}}{2}Q_B^y - \frac{1}{2}Q_B^x\right) + \left(\frac{\sqrt{3}}{2}Q_C^y - \frac{1}{2}Q_C^x\right)\right] \\ Q_y &= \frac{1}{\sqrt{3}}\left[Q_A^y + \left(-\frac{1}{2}Q_B^y + \frac{\sqrt{3}}{2}Q_B^x\right) + \left(-\frac{1}{2}Q_C^y - \frac{\sqrt{3}}{2}Q_C^x\right)\right]. \end{aligned} \tag{22}$$

The action of the group generators on these functions is given by

$$\begin{aligned} \hat{C}_3\begin{pmatrix} Q_x & Q_y \end{pmatrix} &= \begin{pmatrix} Q_x & Q_y \end{pmatrix}\begin{pmatrix} -1/2 & \sqrt{3}/2 \\ -\sqrt{3}/2 & -1/2 \end{pmatrix} \\ \hat{\sigma}_x\begin{pmatrix} Q_x & Q_y \end{pmatrix} &= \begin{pmatrix} Q_x & Q_y \end{pmatrix}\begin{pmatrix} 1 & 0 \\ 0 & -1 \end{pmatrix}. \end{aligned} \tag{23}$$

Note the sign change here as compared to Eq. (20). This is based on the convention that these modes were chosen to mimic the behavior of central quadrupolar harmonics x^2-y^2 and xy, as opposed to the fermion states which follow the dipolar harmonics x and y. With K_e the force constant of the boson mode, and F_e the linear force element, in a fermion basis $\{|x\rangle|y\rangle\}$ the Hamiltonian reads

$$\mathcal{H} = \frac{K}{2}\left(Q_x^2 + Q_y^2\right) + \frac{F_e}{\sqrt{2}}\begin{pmatrix} Q_x & Q_y \\ Q_y & -Q_x \end{pmatrix}. \tag{24}$$

Diagonalization of this Hamiltonian then yields the familiar Mexican hat surface, consisting of two parabolic sheets, with rotational symmetry along the threefold axis:

$$E_\pm = \frac{K}{2}\left(Q_x^2 + Q_y^2\right) \pm \frac{F_e}{\sqrt{2}}\sqrt{Q_x^2 + Q_y^2}\,. \tag{25}$$

The central C_{3v} point of the diagram is unstable, and the energy gain by distortion into the trough is the so-called JT energy, given by

$$E_{JT} = -\frac{1}{2}\frac{F_e^2}{K}\,. \tag{26}$$

If the system rotates around in the trough the nuclei perform circular motions around the trigonal equilibrium positions. This motion is an internal rotation or *libration* as shown in Fig. 5. Additional higher-order terms to the Hamiltonian will essentially maintain the shape of the surface, but introduce warping. As an example, the second-order terms in Q_xQ_y and $Q_x^2 - Q_y^2$ will warp the potential energy surface, giving rise to local hill tops, alternating with local minima. The stationary points correspond to isosceles triangles. Detailed calculations by Cocchini *et al.* [5] for the sodium trimer yield a JT stabilization energy in the order of 670 cm^{-1}, and a rotational barrier of 130 cm^{-1}.

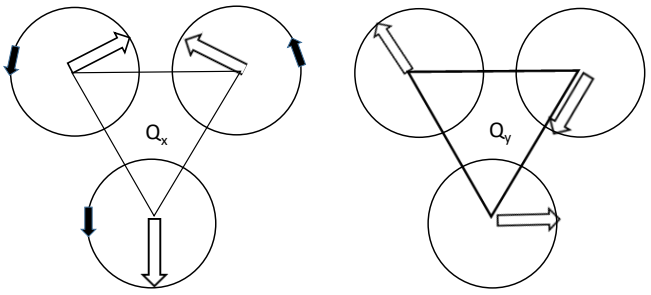

Fig. 5: *Internal rotation along the trough of the Mexican hat; a 90° anti-clockwise rotation takes the Q_x distortion to Q_y.*

2.2 The dynamic system

A fascinating aspect of the Mexican hat potential is certainly its obvious rotational symmetry. This symmetry ultimately goes back to the unitary symmetry of the diabolical degeneracy point at the origin. For a full grasp of this symmetry, we now rewrite the Hamiltonian in its dynamic form, including the nuclear kinetic energy term. According to the standard boson-fermion formalism, the ket functions are generated by the $f_x^\dagger, f_y^\dagger$ operators, and the boson modes are created by $b_x^\dagger, b_y^\dagger$, with coordinate and momentum operators as

$$Q_x = \frac{1}{\sqrt{2}}\left(b_x^\dagger + b_x\right) \quad \text{and} \quad P_x = \frac{i}{\sqrt{2}}\left(b_x^\dagger - b_x\right). \tag{27}$$

A unit of length is defined as $\sqrt{\hbar/m\omega}$ and the oscillator quantum $\hbar\omega$ is taken as the unit of energy. This rescaling absorbs all fundamental constants:

$$\mathcal{H} = \begin{pmatrix} b_x^\dagger b_x + b_y^\dagger b_y + 1 + \kappa\left(b_x^\dagger + b_x\right) & \kappa\left(b_y^\dagger + b_y\right) \\ \kappa\left(b_y^\dagger + b_y\right) & b_x^\dagger b_y + b_y^\dagger b_y + 1 - \kappa\left(b_x^\dagger + b_x\right) \end{pmatrix}. \tag{28}$$

Here, κ is the linear coupling parameter, and 1 is the zero-point energy. *Subsequently this is taken out as the zero of the energy scale.* The angular momentum associated with a rotation in (Q_x, Q_y) is given by

$$\hat{\mathcal{L}}_z = Q_x P_y - Q_y P_x = \frac{i}{2}\Big(\left(b_x^\dagger + b_x\right)\left(b_y^\dagger - b_y\right) - \left(b_y^\dagger + b_y\right)\left(b_x^\dagger - b_x\right)\Big) = i\left(b_y^\dagger b_x - b_x^\dagger b_y\right). \tag{29}$$

To find out the rotational symmetry of the Hamiltonian we calculate the commutator with $\mathcal{L}_z$

$$\left[\hat{\mathcal{L}}_z, \mathcal{H}\right] = i \begin{pmatrix} \kappa\left(b_y^\dagger + b_y\right) & -\kappa\left(b_x^\dagger + b_x\right) \\ -\kappa\left(b_x^\dagger + b_x\right) & -\kappa\left(b_y^\dagger + b_y\right) \end{pmatrix}. \tag{30}$$

Unexpectedly perhaps, the two operators do not commute! However we should be aware that the Hamiltonian describes a coupled situation where both boson and fermion fields are affected. To this aim, we introduce an angular coordinate ϕ in distortion space, with $Q_x = Q\cos\phi$

and $Q_y = Q\sin\phi$. The ground state wavefunction (with $\kappa<0$) of the static Hamiltonian as a function of ϕ is given by

$$|\psi_-\rangle = \cos\frac{\phi}{2}\,|x\rangle + \sin\frac{\phi}{2}\,|y\rangle. \tag{31}$$

This shows the rotation of the wavefunction along the trough, but at half speed as compared to the coordinate change. The wavefunction provides a connection between a base space, providing the real distortions of the system, and a function space, which for every point in the base space, gives a fermion vector. As the boson vector is a direct product of the fermion vector (remember $e \in [E\times E]$), we can qualify the fermion space as a fundamental spin space, and the boson space on top of that as a coupled vector space. The geometry of this connection will be examined in the next section. Here it suffices to define a rotation operator for the fermion states in analogy with the pseudo-spin operator $\mathcal{S}_z$

$$\hat{\mathcal{S}}_z = \frac{i}{2}\big(f_y^\dagger f_x - f_x^\dagger f_y\big). \tag{32}$$

Pursuing this analogy with spin-orbit coupling further, we can define the total momentum operator as $\hat{\mathcal{J}}_z$ by

$$\hat{\mathcal{J}}_z = \hat{\mathcal{L}}_z + \hat{\mathcal{S}}_z\,. \tag{33}$$

This sum operator commutes with the Hamiltonian, as the sum of the commutator of $\hat{\mathcal{S}}_z$ and the commutator with the boson part cancels out: $[\mathcal{S}_z,\mathcal{H}] = -[\mathcal{L}_z,\mathcal{H}]$. In order to take advantage of the conservation of angular momentum, we now impose symmetry adapted combinations of bosons and fermions. One has

$$b_\pm^\dagger = \frac{1}{\sqrt{2}}\left(b_x^\dagger \pm i b_y^\dagger\right) \quad \text{and} \quad b_\pm = \frac{1}{\sqrt{2}}\left(b_x \mp i b_y\right). \tag{34}$$

These operators are eigenoperators of $\hat{\mathcal{L}}_z$ with opposite eigenvalues

$$\left[\hat{\mathcal{L}}_z, b_\pm^\dagger\right] = \pm b_\pm^\dagger \quad \text{and} \quad \left[\hat{\mathcal{L}}_z, b_\pm\right] = \mp b_\pm\,. \tag{35}$$

Analogous symmetry adaptation of the fermion operators yields

$$|\uparrow\rangle = \frac{1}{\sqrt{2}}\big(|x\rangle + i|y\rangle\big) \quad \text{and} \quad |\downarrow\rangle = \frac{1}{\sqrt{2}}\big(|x\rangle - i|y\rangle\big). \tag{36}$$

As eigenfunctions of the $\hat{\mathcal{S}}_z$ operator, these combinations are like α and β spins

$$\hat{\mathcal{S}}_z|\uparrow\rangle = +\frac{1}{2}|\uparrow\rangle \quad \text{and} \quad \hat{\mathcal{S}}_z|\downarrow\rangle = -\frac{1}{2}|\downarrow\rangle. \tag{37}$$

The total symmetry-adapted Hamiltonian is now expressed in the transformed fermion basis

$$\begin{pmatrix} |\uparrow\rangle \\ |\downarrow\rangle \end{pmatrix}: \qquad \mathcal{H} = \begin{pmatrix} b_+^\dagger b_+ + b_-^\dagger b_- & \kappa\sqrt{2}\big(b_-^\dagger + b_+\big) \\ \kappa\sqrt{2}\big(b_+^\dagger + b_-\big) & b_+^\dagger b_+ + b_-^\dagger b_- \end{pmatrix}. \tag{38}$$

To solve this Hamiltonian equation it is of paramount importance to define an Ansatz. An Ansatz is a general expression of the form of the solution, which holds the symmetry of the

system, and expresses the coupling scheme between the boson and fermion degrees of freedom. The Ansatz reads

$$|\Psi\rangle_{l+1/2} = \left(b_+^\dagger\right)^l \Phi_1(\xi)\,|\uparrow\rangle + \left(b_+^\dagger\right)^{l+1} \Phi_2(\xi)\,|\downarrow\rangle. \tag{39}$$

Here the variable ξ is defined as

$$\xi = b_+^\dagger b_-^\dagger. \tag{40}$$

This variable thus corresponds to a two-photon boson excitation, combing two excitations with opposite angular momentum. The total angular momentum of this variable is thus equal to zero, and it can be considered as a double purely radial excitation. The Ansatz shows that in order to obtain a vibronic state with angular momentum $l+1/2$, on top of an arbitrary number of radial excitations we can either excite l quanta of $b_+^\dagger$ and couple this to a spin-up fermion state, or excite $l+1$ quanta of $b_+^\dagger$ and couple this with a spin-down fermion. These are the only two channels to arrive at a state with the desired momentum. This state will always be degenerate with a time-reversed counterpart, which is given by

$$|\Psi\rangle_{-l-1/2} = \left(b_-^\dagger\right)^l \Phi_1(\xi)\,|\downarrow\rangle + \left(b_-^\dagger\right)^{l+1} \Phi_2(\xi)\,|\uparrow\rangle. \tag{41}$$

The Ansatz clearly shows that the vibronic wavefunction cannot be factorized as a product of a fermion and a boson part: we have definitely taken leave from the Born-Oppenheimer approximation. In summary the JT equations to be solved read in matrix form

$$\mathcal{H}|\Psi\rangle = E|\Psi\rangle = \begin{pmatrix} b_x^\dagger b_x + b_y^\dagger b_y + \kappa\left(b_x^\dagger + b_x\right) & \kappa\left(b_y^\dagger + b_y\right) \\ \kappa\left(b_y^\dagger + b_y\right) & b_x^\dagger b_y + b_y^\dagger b_y - \kappa\left(b_x^\dagger + b_x\right) \end{pmatrix} \begin{pmatrix} \left(b_+^\dagger\right)^l & \Phi_1(\xi) \\ \left(b_+^\dagger\right)^{l+1} & \Phi_2(\xi) \end{pmatrix}. \tag{42}$$

We refer to [1] for a detailed discussion of the solution of these equations. Interestingly the equations can ultimately be turned into a form of Heun's differential equation. Closed solutions of this equation do not seem to exist, except for some special values of κ. Eigenvalues are characterized by half integral values of j and are plotted as a function of the coupling parameter, in close-up in Fig. 6.

At the left of the diagram, for $\kappa = 0$, are found the oscillator levels of the e-vibration. When the coupling sets in, the trough develops, and ultimately – in the strong coupling limit – the spectrum reduces to a rotational spectrum with a regular sequence of half-integral j-values, superimposed on a transversal oscillator. Looking in detail at the lowest vibronic levels, in the limit of zero coupling strength the ground level with $j = 1/2$ reduces to the product of the electronic degeneracy and the totally-symmetric zero phonon state. The excited oscillator state at $E = 1$ corresponds to the vector addition of an $l = 1$ vibrational level to the fermion spin, yielding $j = 1/2,\, 3/2$. As the coupling is turned on, the $j = 1/2$ excited state is raised due to its interaction with the equisymmetric ground state, while the $j = 3/2$ level is expected to descent in energy, as seen in the figure.

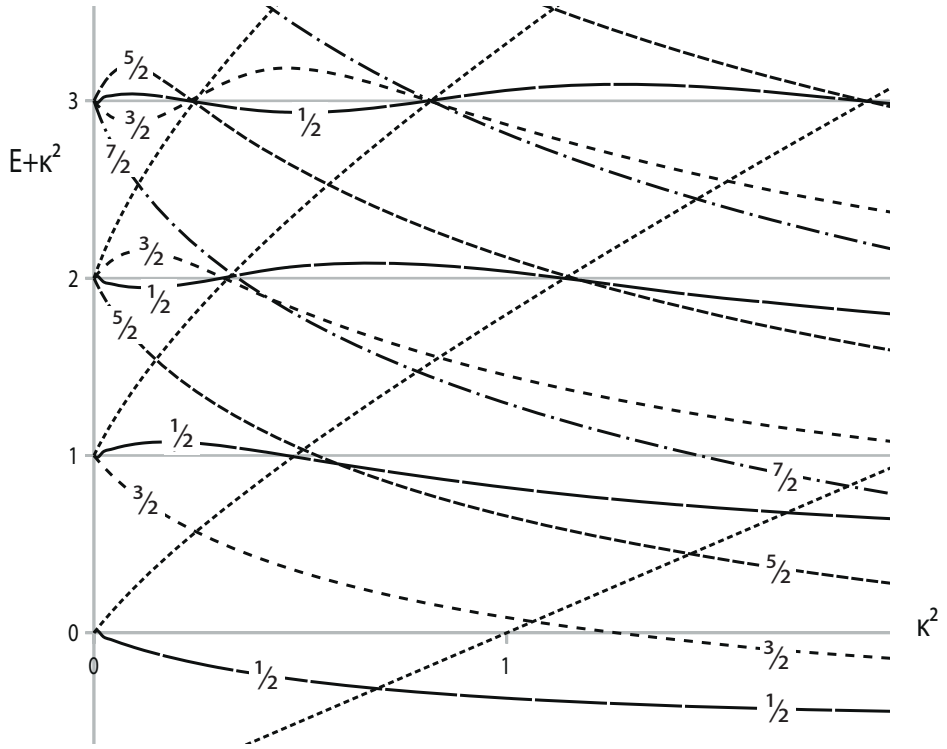

Fig. 6: *$E \times e$ JT Hamiltonian: solutions of the dynamic equation as a function of κ^2; individual lines are characterized by angular momentum j; ascending dotted lines represent extra mathematical solutions that are unphysical.*

If quadratic warping terms are introduced, the rotational symmetry is broken to C_{3v}. Accordingly, the j states subduce trigonal levels as indicated below

$$\begin{aligned} j = 1/2 &\rightarrow E \\ j = 3/2 &\rightarrow A_1 + A_2 \,. \end{aligned} \tag{43}$$

In a strong coupling regime with extensive trigonal warping, the vibronic regime in essence reduces to local oscillations in three localized wells. Depending on the signs of the warping parameters, the minima are either at $\phi = 0°, 120°, 240°$ with saddle points in between, or vice-versa. Small vibrational overlap between these wells opens the possibility of tunneling.The lowest tunneling states are obtained by setting up a 3×3 hopping matrix between the wells. The matrix element between the wells essentially is a Huang-Rhys overlap factor, with a positive sign. The result is a two state diagram, with an E ground state, and an A excited state, which are separated by a tunneling splitting. Here the lower E state correlates with the ground $j = 1/2$ level of the diagram. The upper A state correlates likewise with the $j = 3/2$ parentage. As Eq. (43) shows, it can be either A_1 or A_2. For wells located at turning points $0°, 120°, 240°$, the A level is identified as an A_1 level. When the surface is turned upside down, with minima now at $60°, 180°, 300°$, the A level has A_2 symmetry. These results follow from the electronic part of the wavefunction in Eq. (31), as the vibrational overlap is symmetric with respect to reflections in C_{3v} [6].

2.3 Berry phase

We already drew attention to the sign change of the wavefunction after revolving around the conical intersection. The acquired phase is a geometric phase, which is generally known as a Berry phase, following the seminal work of Michael Berry [7]. Berry's phase was identified with the concept of holonomy in geometry. To present this concept, two ingredients are required: the base space, and the fiber. In the JT case the base space is the coordinate space $\{Q_x, Q_y\}$ formed by the two distortion modes. With each point in the base space a wavefunction can be associated. The phase of this wavefunction may vary over a range $0, 2\pi$. The phase variable forms a so-called fiber, associated with a particular point on the base space. The collection of all these fibers over the entire base space forms a fiber bundle. Now the holonomy is what we observe in the fiber bundle when a closed loop is performed in the base space. Clearly, in order to be meaningful, a connection must exist which controls the change of the phase in consecutive fibers, corresponding to adjacent points on the base space. Berry showed how this connection is provided by the time-dependent Schrödinger equation, under adiabatic constraints. This is fulfilled in the case of a circuit driven by slowly moving nuclei along the trough of the potential, with instantaneous adaptation of the wavefunction, not involving excitations. Ideally we may think of a slow rotation which is hindered by the surface warping along the circuit. The treatment proceeds as follows: let $|n(\mathbf{R})\rangle$ represent the non-degenerate quantum state of a system, dependent on external parameters $\mathbf{R}$, which corresponds to a particular nuclear configuration along the low-energy trough. The eigenvalue is given by

$$\mathcal{H}(\mathbf{R})|n(\mathbf{R})\rangle = E_n(\mathbf{R})|n(\mathbf{R})\rangle. \tag{44}$$

The wavefunction $|n(\mathbf{R})\rangle$ must be *single valued* in the relevant parameter domain, and be *differentiable*. The wavefunction which solves the time-dependent Schrödinger equation in the adiabatic regime is then given by

$$|\Psi\rangle = \exp\left(-\frac{iE_n}{\hbar}t\right)|n(\mathbf{R})\rangle. \tag{45}$$

Here a time-dependent phase factor, the so-called dynamical phase, is added. This factor measures the passage of time. In the JT application we consider a closed circuit, C, in a space defined by nuclear displacements, $\mathbf{R}(t)$, where the distortion varies smoothly and slowly in time, as the nuclei evolve on a minimal energy path. Since the adiabatic state depends on the coordinates, it will change accordingly, but continuously, i.e., the Hamiltonian does not change rapidly enough to allow excitations to other states with energy $E_m(\mathbf{R})$. Nonetheless, by slowly driving the state around in the distortion space, an extra time dependence will appear, as is evident from the notation $|n(\mathbf{R}(t))\rangle$. In order to keep satisfying the time dependent equation, we must include a further compensatory phase factor. Eq. (45) is thus rewritten as

$$|\Psi\rangle = \exp\left(-\frac{iE_n}{\hbar}t\right)\exp\Big(i\gamma_n(t)\Big)|n(\mathbf{R}(t))\rangle. \tag{46}$$

Here the second exponential represents the geometric phase that is at the core of Berry's treatment. Applying the time dependent equation yields

$$i\hbar\frac{d}{dt}\,|\Psi\rangle = E_n|\Psi\rangle - \hbar\frac{d\gamma_n}{dt}\,|\Psi\rangle + i\hbar\exp\left(-\frac{iE_n}{\hbar}t\right)\exp\Big(i\gamma_n(t)\Big)\frac{d}{dt}|n(\mathbf{R}(t))\rangle. \tag{47}$$

In order to satisfy the Schrödinger equation, one must require that the sum of the second and third terms cancel

$$-\frac{d\gamma_n}{dt}|\Psi\rangle + i\exp\left(-\frac{iE_n}{\hbar}t\right)\exp\Big(i\gamma_n(t)\Big)\frac{d}{dt}|n(\mathbf{R}(t))\rangle = 0\,. \tag{48}$$

This can be rewritten as

$$d\gamma_n = i\langle n(\mathbf{R})|dn(\mathbf{R})\rangle = i\langle n(\mathbf{R})|\nabla_R|n(\mathbf{R})\rangle\cdot\mathrm{d}\mathbf{R} \tag{49}$$

When completing a closed loop, the total build-up of the phase is measured by the line integral along the path

$$\gamma_n(C) = \oint_C d\gamma_n = i\oint\langle n|dn\rangle, \tag{50}$$

with $|dn\rangle = \nabla_R|n\rangle\cdot\mathrm{d}\mathbf{R}$. Furthermore since the ket function is normalized, one has

$$d\langle n|n\rangle = \langle dn|n\rangle + \langle n|dn\rangle = \overline{\langle n|dn\rangle} + \langle n|dn\rangle = 0\,. \tag{51}$$

This implies that the matrix element $\langle n|dn\rangle$ is purely imaginary, and thus that $\gamma_n(C)$ will be real. This integral is the famous Berry phase. If the path is defined on a curved surface this phase will be non-trivial. In order to apply this treatment to the JT system, it is first of all noted that the electronic wavefunction $|\psi_-\rangle$ given in Eq. (31) is not single-valued, since

$$|\psi_-(2\pi)\rangle = \exp(i\pi)|\psi_-(0)\rangle. \tag{52}$$

So $|\psi_-\rangle$ does not correspond to $|n(\mathbf{R})\rangle$. However, by gradually removing the phase of π during the circuit, we obtain the required single-valued function

$$|n(\mathbf{R})\rangle = \exp\left(-\frac{i\phi}{2}\right)|\psi_-(\phi)\rangle = \exp\left(-\frac{i\phi}{2}\right)\Big(\cos\phi/2|E_x\rangle + \sin\phi/2|E_y\rangle\Big). \tag{53}$$

And thus

$$\begin{aligned} d|n(\mathbf{R})\rangle &= \exp\left(-\frac{i\phi}{2}\right)\left(-\frac{id\phi}{2}|\psi_-(\phi)\rangle + d|\psi_-(\phi)\rangle\right) \\ \langle n(\mathbf{R})|dn(\mathbf{R})\rangle &= -\frac{i\,d\phi}{2}\,. \end{aligned} \tag{54}$$

Here we made use of the fact that $|\psi_-\rangle$ is real, and hence

$$d\langle\psi|\psi\rangle = 2\langle\psi|d\psi\rangle = 0\,. \tag{55}$$

Inserting the result in Eq. (50) yields

$$\gamma_n(C) = \oint_C d\gamma_n = i\oint\langle n|dn\rangle = i\oint\Big(-\frac{i}{2}\Big)d\phi = \pi\,. \tag{56}$$

As Berry writes, *one might say that the dynamical phase factors in Eq.* (45) *and* γ_n *in Eq.* (46) *give the system's best answers to two questions about its adiabatic circuit. For the dynamical phase the question is: how long did your journey take? For* $\gamma_n(C)$ *it is: where did you go to?* Here we open a brief parenthesis: as the integral $\langle\psi|d\psi\rangle$ is zero, the function $|\psi\rangle$ is said to follow the law of parallel transport. It means that the change of the function is orthogonal to the function itself. This implies that the function accumulates during its path the torsion that is forced upon the system by the path, and as a result its end state after a full circuit will end up with a net phase difference. Following a function under parallel transport and detecting the phase change after a full circuit is thus a direct way to obtain the Berry phase.
Now what are the implications of the Berry phase for the JT treatment? In Eq. (49) it is noted that the gradient element adds an extra phase to the wavefunction, exactly as the vector potential $\mathbf{A}$ does to a charged particle in magnetism. In view of this analogy, we may introduce a vector field terminology, and write

$$\mathbf{A} = i\langle n(\mathbf{R})|\nabla_R|n(\mathbf{R})\rangle \tag{57}$$

and

$$\gamma_n(C) = \oint_C \mathbf{A}\cdot \mathrm{d}\mathbf{R}\,. \tag{58}$$

$\mathbf{A}$ lives in parameter space, and emanates from the topology of this space. As it is dependent on the phase of the basis vectors, it is not unique, and when applying the formula in Eq. (57), one must make sure that the basis vector is locally single-valued. In the JT case working out these expressions yields

$$A_\phi = i\big\langle n\big|\,\frac{\delta}{\delta\phi}\,\big|n\big\rangle = \frac{1}{2}\,. \tag{59}$$

The form of this vector potential is analogous to the field created by a Dirac monopole of strength $1/2$. The source of this monopole is nothing else than the conical intersection itself. The question thus arises if the dynamic calculations which we performed indeed include the vector potential associated with the conical intersection, or if an additional field term in the Hamiltonian is required. The short answer is that the dynamic treatment, which we have presented, does indeed contain the Berry phase from the start, so there was no need to invoke it afterwards. This being said, the literature hardly offers explicit demonstrations of this correspondence. An exception is the treatment by Johnsson and Stedman [8]. To spell out the angular momentum of the nuclear motion in the presence of a vector field, we must include the term $-q\mathbf{A}$ in the vector product $\mathbf{R}\wedge\mathbf{P}$

$$\mathbf{R}\wedge(\mathbf{P}-q\mathbf{A}) = \mathcal{L} - q\frac{1}{2} = \mathcal{J}_z\,, \tag{60}$$

where $q = \pm 1$ is the charge of the particle. The fact that we recover the angular momentum operator of the dynamic JT treatment indicates that this treatment indeed fully incorporates the Berry phase. The angular momentum thus truly reflects the dual boson-fermion characteristic of the JT Hamiltonian.

3 The triplet $T \times (e + t_2)$ Jahn-Teller system

Triple degeneracies occur in cubic and icosahedral symmetries. The symmetries of the JT modes are generated as

$$\begin{aligned} O_h &: [T \times T] - A_{1g} = e_g + t_{2g} \\ I_h &: [T \times T] - A_g = h_g \end{aligned} \tag{61}$$

T-terms have a frequent occurrence in coordination compounds and metal clusters, often with important implications for magnetism. The strength of the coupling is usually less pronounced than for E-terms, giving rise to all sorts of dynamic properties. A notable example of an icosahedral T-system is the ground state of the fulleride anion, C_{60}^{-}, due to the occupation of the t_{1u} LUMO of Buckminsterfullerene by a single electron.

3.1 The Hamiltonian

As before two spaces are to be considered: the fermion basis defines a three-dimensional sphere, with unit vectors $|T_x\rangle, |T_y\rangle, |T_z\rangle$, and the boson space, forming a five-dimensional Euclidean space, with unit vectors Q_θ, Q_ϵ for the e_g-modes and Q_ξ, Q_η, Q_ζ for the t_{2g}-modes.
In the linear coupling regime, the Hamiltonian is given by

$$\mathcal{H} = \frac{1}{2}K_E\left(Q_\theta^2 + Q_\epsilon^2\right) + \frac{1}{2}K_{T_2}\left(Q_\xi^2 + Q_\eta^2 + Q_\zeta^2\right) + \mathcal{H}' \tag{62}$$

with

$$\mathcal{H}' = F_E \begin{pmatrix} -\frac{1}{2}Q_\theta + \frac{\sqrt{3}}{2}Q_\epsilon & 0 & 0 \\ 0 & -\frac{1}{2}Q_\theta - \frac{\sqrt{3}}{2}Q_\epsilon & 0 \\ 0 & 0 & Q_\theta \end{pmatrix} + \frac{F_{T_2}}{\sqrt{2}} \begin{pmatrix} 0 & -Q_\zeta & -Q_\eta \\ -Q_\zeta & 0 & -Q_\xi \\ -Q_\eta & -Q_\xi & 0 \end{pmatrix}. \tag{63}$$

The potential energy surface is defined in 5D coordinate space. However a concise view of the topography of the surface can be achieved by projection in 3D fermion space. The procedure is as follows: consider an electronic eigenvector (x, y, z), normalized to unity

$$|T(\mathbf{r})\rangle = x|T_x\rangle + y|T_y\rangle + z|T_z\rangle. \tag{64}$$

Antipodal points (x, y, z) and $(-x, -y, -z)$ describe the same solution, hence the electronic space is restricted to a hemisphere. This surface has the topology of a projective plane. Now minimize the energy for every direction on this sphere

$$\frac{\delta}{\delta Q_{\Lambda\lambda}}\left(\mathbf{r}^\dagger \mathcal{H} \mathbf{r}\right) = \mathbf{r}^\dagger \frac{\delta \mathcal{H}}{\delta Q_{\Lambda\lambda}} \mathbf{r} = 0 \qquad \forall\ Q_{\Lambda\lambda} \in [\Gamma]^2 - \Gamma_0\,. \tag{65}$$

This yields a set of equations from which we may determine the stationary coordinates, denoted as $\|Q_{\Lambda\lambda}\|_r$. Reinserting these coordinates in the energy expressions yields the function $\|E\|_r$. This function does not represent eigenenergies, except in the stationary points where it is indeed

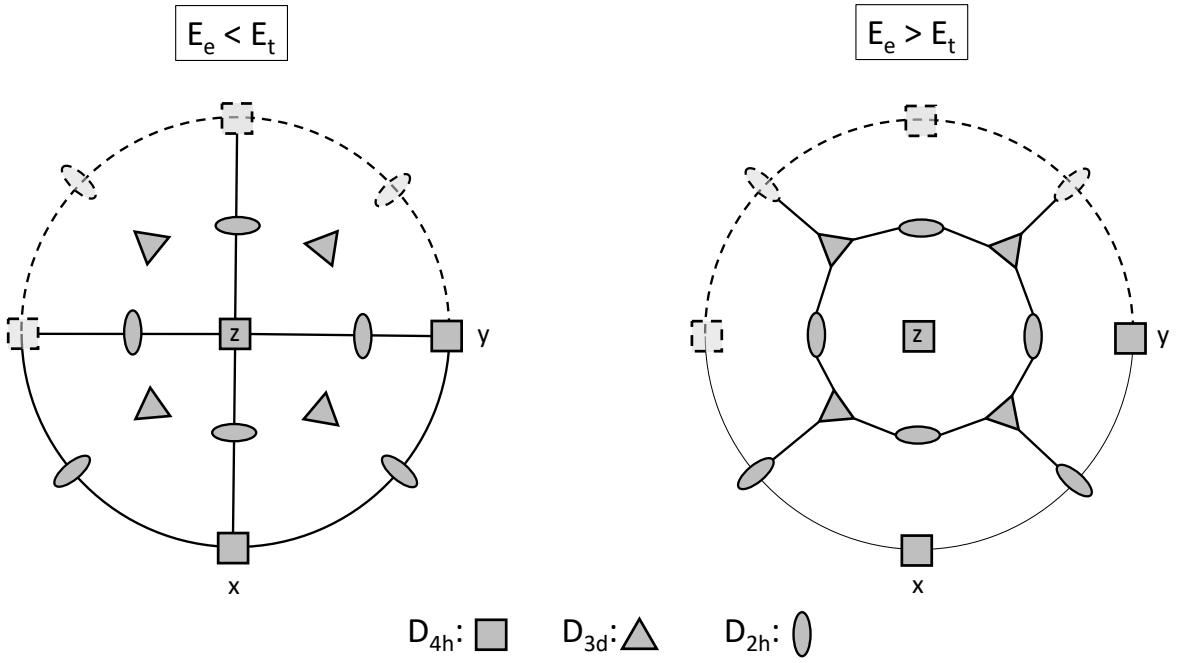

Fig. 7: *Jahn-Teller distortions for a cubic triplet, projected on a hemisphere; the z-axis is the upright axis.*

a root of the matrix equation! Hence this function is *isostationary*, i.e., it coincides with the hypersurface in the stationary points. As an example, for the cubic T-terms, the isostationary function is given by

$$\langle \|E\| \rangle_{\mathbf{r}} = \frac{1}{5}\big(2E_E^{JT}+3E_{T_2}^{JT}\big) + \frac{6}{5}\big(E_E^{JT}-E_{T_2}^{JT}\big) f_4 \tag{66}$$

with

$$E_E^{JT} = -\frac{1}{2}\frac{F_E^2}{K_E} \qquad E_{T_2}^{JT} = -\frac{1}{3}\frac{F_{T_2}^2}{K_{T_2}} \qquad f_4 = \frac{1}{2}\Big(x^4+y^4+z^4 - 3\left(x^2y^2+x^2z^2+y^2z^2\right)\Big). \tag{67}$$

The f_4 polynomial, which controls the topography, is recognized here as the cubic invariant of the fourth-order spherical harmonics, which also provides the crystal field potential in octahedral symmetry. The term preceding f_4 involves the difference of the JT stabilization energies. If the stabilization along e-modes is more pronounced, the surface is characterized by tetragonal minima, with orthorhombic saddle points in between. The trigonal extrema in this case are hill tops on the surface. In contrast if the t_2-modes prevail, the surface will be turned upside down, as shown in Fig. 7. Additional second-order terms in the Hamiltonian will produce a further warping of the surface. As an example, when both e and t_2 modes are active, and there is a strong second-order interaction term between them, the next cubic invariant of rank 6 will take over control, and produce a surface with six orthorhombic D_{2h} minima and twelve C_{2h} saddle points in between.

In the icosahedral case the linear JT Hamiltonian is isotropic and the hypersurface corresponds to a 3D sphere. However upon introduction of second-order warping terms minima and maxima

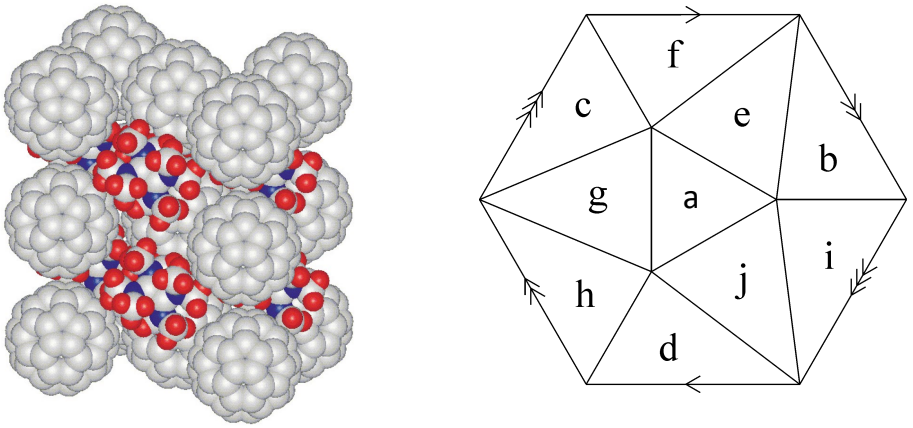

Fig. 8: *Jahn-Teller distortions for an isosahedral triplet, in a projective plane, consisting of six vertices and ten triangular faces: the vertices correspond to D_{5d} points, and the faces to D_{3d} points; left is shown the crystal structure of TDAE$^{+}C_{60}^{-}$ (taken from [9]).*

appear. These are governed by an icosahedral invariant of rank 6. Again two regimes are possible: either ten trigonal minima, and six pentagonal hill tops, or vice-versa. The pentagonal points are all equidistant and form the complete graph of six nodes. The nine neighbors of each trigonal point split into two orbits of orders three and six. A case in point is the anion of C_{60}. Fulleride ions may be formed by reduction with alkali metals, or electron donors such as tetrakis(dimethylamino)ethylene [9] TDAE, see Fig. 8.

3.2 Dynamics

For an understanding of the dynamics we turn to the high-symmetry case, where the Hamiltonian is limited to the linear force elements, and with – in case of cubic symmetry – degenerate coupling between e and t_2 modes: $E_e^{JT} = E_{t_2}^{JT}$. As the isostationary function demonstrates, the potential energy minimum in this case forms a continuum. This corresponds to a 3D spherical trough in the 5D coordinate space. In analogy to the circular motion of atoms in the JT-trough for a triangle shown before in Fig. 5, in the present case of a spherical trough the loci of displacements of individual atoms form a sphere, centered at their high-symmetry positions. Judd has provided a detailed analysis of this internal rotation in the case of a T-type JT surface in an octahedron [10]. The motions of equivalent atoms are locked and concerted so that the total degree of freedom corresponds to the symmetry group of a 3D sphere, which is the special orthogonal group in 3D: $SO(3)$.

The Hamiltonian for the highly symmetric limit, also known as the $P \times d$ Hamiltonian, describes the coupling between a dipolar fermion part and its symmetrized square which corresponds to a quadrupolar tensor. It consists of a harmonic part, $\mathcal{H}_0$, and the standard linear coupling term, $\mathcal{H}'$, which is the scalar product of the fermion tensor and the coordinate tensor

$$\mathcal{H}' = k \sum_q (-1)^q (\mathbf{f}^\dagger \mathbf{f})_q^2 Q_{-q} \,. \tag{68}$$

Here k is the coupling parameter. The coordinates are written in their complex format, defined

as

$$Q_0 = Q_\theta\ , \quad Q_{\pm1} = \mp\frac{1}{\sqrt{2}}Q_\eta - \frac{i}{\sqrt{2}}Q_\xi \quad \text{and} \quad Q_{\pm2} = \frac{1}{\sqrt{2}}Q_\epsilon \pm \frac{i}{\sqrt{2}}Q_\zeta\,. \tag{69}$$

In matrix form, acting in the space of the fermions, ordered as $|{+1}\rangle, |\ 0\ \rangle, |{-1}\rangle$, the coupling Hamiltonian reads

$$\mathcal{H}' = k\begin{pmatrix} \frac{1}{\sqrt{6}}Q_0 & \frac{1}{\sqrt{2}}Q_{-1} & Q_{-2} \\ -\frac{1}{\sqrt{2}}Q_{+1} & -\frac{2}{\sqrt{6}}Q_0 & -\frac{1}{\sqrt{2}}Q_{-1} \\ Q_{+2} & \frac{1}{\sqrt{2}}Q_{+1} & \frac{1}{\sqrt{6}}Q_0 \end{pmatrix}. \tag{70}$$

As this is a scalar product of spherical tensors, the coupling Hamiltonian will be $SO(3)$ invariant. The secular equation of $\mathcal{H}'$ reduces to

$$E^3 - \frac{E}{2}Q^2 + \frac{1}{3\sqrt{6}}I_3^3 = 0 \tag{71}$$

where

$$\begin{aligned} Q^2 =& Q_0^2 - 2Q_{+1}Q_{-1} + 2Q_{+2}Q_{-2} \\ I_3 =& Q_0\big(Q_0^2 - 6Q_{+2}Q_{-2} - 3Q_{+1}Q_{-1}\big) + \frac{3\sqrt{3}}{\sqrt{2}}\big(Q_{+2}Q_{-1}^2 + Q_{-2}Q_{+1}^2\big). \end{aligned} \tag{72}$$

The interesting aspect of this secular equation is that it contains two $SO(3)$ invariants: Q is the squared norm of the distortion space and thus measures the extent of the distortion, while I_3 is a third-order invariant, proportional to the determinant of the JT Hamiltonian. The roots of the eigenvalue equation can be expressed using the angle representation. Rewrite I_3 as:

$$I_3 = Q^3 \cos 3\gamma\,. \tag{73}$$

The equation can then easily be solved by the trigonometric expressions for the three roots

$$E_k = -kQ\frac{2}{\sqrt{6}}\cos\left(\gamma - \frac{2n\pi}{3}\right)\ n = 0, 1, 2. \tag{74}$$

What is the meaning of the angle γ which appears when solving the secular equation? The answer to this question takes us to the 5D oscillator formed by the quadrupolar Q_{m_l} JT modes. The parent symmetry of the 5D oscillator is the special unitary group $SU(5)$ which allows for all possible unitary transformations of the five quadrupolar modes. This group can conveniently be restricted to its subgroup of orthogonal transformations, $SO(5)$. However, when considering the JT Hamiltonian, symmetry is restricted to an even lower subgroup, corresponding to the sphere in 3D, with symmetry group $SO(3)$. A clear understanding of the embedding of $SO(3)$ in $SO(5)$ is offered by the surface oscillations of a vibrating sphere, which have been studied extensively in nuclear physics as a model for the vibrating nucleus. Low-energy nuclear vibrations indeed match the five quadrupolar modes (and likewise for the tidal waves on earth), dipoles being removed as they correspond to spurious translations. On the other hand the totally symmetric scalar mode, which corresponds to a breathing mode, is way higher in energy, since it stretches the surface everywhere. Besides, in the JT context it is inactive as it doesn't break

the symmetry. The model of the vibrating hollow sphere thus provides a complete description of the quadrupolar modes. Since the quadrupolar modes have the smallest allowed L value, they can only introduce a minimal symmetry breaking: they distort a sphere into an ellipsoid. An ellipsoid is a surface characterized by three orthogonal axes of different length. The sum of these lengths must be constant in time, in order to avoid any admixture of the radial breathing mode. Hence proper ellipsoidal distortions have only two degrees of freedom. These correspond to the tetragonal Q_θ mode and the orthorhombic Q_ϵ mode. The tetragonal mode leads to a prolate ($Q_\theta > 0$) or oblate ($Q_\theta < 0$) ellipse, which still has cylindrical symmetry along the z-axis. The radius of this ellipse is thus described as

$$d(\theta, \phi) = R\big(1 + c(3\cos^2\theta - 1)\big), \tag{75}$$

where R is the radius of the sphere, and c is scaling constant which oscillates in time with the vibration. The orthorhombic mode will further break this axial symmetry, by repartitioning the distortion between the x- and y- directions. A general ellipsoidal distortion with principal axes along the Cartesian directions is thus described by a vector in the space formed by these two coordinates. This is a bimodal distortion [11]. Turning to polar coordinates, the parametric description of this distortion reads

$$\begin{pmatrix} Q_\theta \\ Q_\epsilon \\ Q_\xi \\ Q_\eta \\ Q_\zeta \end{pmatrix} = Q \begin{pmatrix} \cos\gamma \\ \sin\gamma \\ 0 \\ 0 \\ 0 \end{pmatrix}. \tag{76}$$

The angle which appears here refers to the balance between tetragonal and orthorhombic modes, and this is precisely the angle γ which appeared in the secular equation. The ellipsoid which is obtained by this bimodal distortion is still aligned with the Cartesian reference frame. Spherical symmetry of course requires that the ellipsoid is free to rotate in 3D space. This is where the three remaining quadrupolar modes come in. The general orientation of the ellipsoidal distortion can be performed by the Euler rotation matrix in the full space of the five L=2 modes. In summary a symmetry adaptation has been performed of the five degrees of freedom: three angles describe the orientation in 3D space and present the spherical $SO(3)$ symmetry of the vibrating sphere. A radius and an extra angle γ define the ellipsoidal distortion. As this extra angular degree of freedom appears in the secular equation, the total Hamiltonian has only $SO(3)$ symmetry, and does not form a spherical surface in 5D. The T-term JT problem is thus at its core a symmetry breaking chain $SU(5) \downarrow SO(5) \downarrow SO(3)$. The relevant irreducible representations (irreps) for each of these groups are as follows:

- Excitations of n oscillator quanta in $SU(5)$ correspond to irrep $[n]$.
- Relevant irreps in $SO(5)$ are denoted as $(\nu, 0)$. Here ν is a whole number, which is known as the Racah seniority number.
- Irreps in $SO(3)$ are characterized by the angular momentum quantum number L.

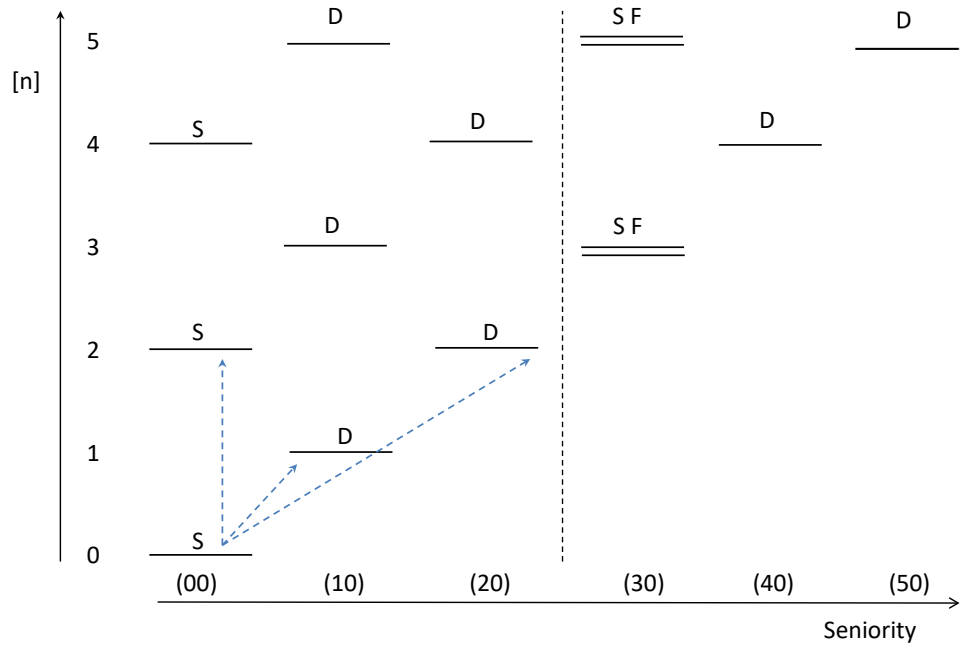

Fig. 9: *3D assignments of the surface vibrations of a sphere; the vertical axis represents the oscillator states of a 5D oscillator; the horizontal axis decomposes these states in $SO(5)$ seniorities; spherical components are indicated by S,D,F,... angular momentum; note the repetition of the SDD pattern, with a period of three.*

The branching scheme along the symmetry lowering chain is shown in Fig. 9. It represents the energy of the boson spectrum at zero JT coupling. As the coupling sets in, the L levels are coupled with the P fermion level, according to the usual vector addition rules. As an example, in order to realize a vibronic state with P symmetry, only S and D levels are involved: $S{\times}P = P$ and $D{\times}P = P{+}D{+}F$. Interestingly the diagram shows that the initial SDD pattern shows a perfect repetition with a period of three. This observation allows to construct an Ansatz, with spherical symmetry and the two extra-spherical degrees of freedom which appear in the secular equation: the radius Q which measures the vertical radial excitations in the diagram, and the angle γ which takes us through the horizontal seniority period in the diagram. We conclude by providing the Ansatz

$$\Psi_0 = \begin{pmatrix} \left(\quad \sqrt{3}b^\dagger_{-1}\mathcal{F}_1 \quad +(\mathbf{b}^\dagger\mathbf{b}^\dagger)^2_{-1}\mathcal{F}_2\right) f^\dagger_{+1} \\ \left(\mathcal{F}_0 - 2b^\dagger_0\,\mathcal{F}_1 \quad -2(\mathbf{b}^\dagger\mathbf{b}^\dagger)^2_0\,\mathcal{F}_2\right) f^\dagger_0 \\ \left(\quad \sqrt{3}b^\dagger_{+1}\mathcal{F}_1 + \sqrt{6}(\mathbf{b}^\dagger\mathbf{b}^\dagger)^2_{+1}\mathcal{F}_2\right) f^\dagger_{-1} \end{pmatrix} \qquad \text{and}$$

$$\Psi_{+1} = \begin{pmatrix} \left(\mathcal{F}_0 \quad +b^\dagger_0\,\mathcal{F}_1 \quad +(\mathbf{b}^\dagger\mathbf{b}^\dagger)^2_0\,\mathcal{F}_2\right) f^\dagger_{+1} \\ \left(\quad -\sqrt{3}b^\dagger_{+1}\mathcal{F}_1 - \sqrt{3}(\mathbf{b}^\dagger\mathbf{b}^\dagger)^2_{+1}\mathcal{F}_2\right) f^\dagger_0 \\ \left(\quad \sqrt{6}b^\dagger_{+2}\mathcal{F}_1 + \sqrt{6}(\mathbf{b}^\dagger\mathbf{b}^\dagger)^2_{+2}\mathcal{F}_2\right) f^\dagger_{-1} \end{pmatrix}, \; \Psi_{-1} = \begin{pmatrix} \left(\quad \sqrt{6}b^\dagger_{-2}\mathcal{F}_1 + \sqrt{6}(\mathbf{b}^\dagger\mathbf{b}^\dagger)^2_{-2}\mathcal{F}_2\right) f^\dagger_{+1} \\ \left(\quad -\sqrt{3}b^\dagger_{-1}\mathcal{F}_1 - \sqrt{3}(\mathbf{b}^\dagger\mathbf{b}^\dagger)^2_{-1}\mathcal{F}_2\right) f^\dagger_0 \\ \left(\mathcal{F}_0 \quad +b^\dagger_0\,\mathcal{F}_1 \quad +(\mathbf{b}^\dagger\mathbf{b}^\dagger)^2_0\,\mathcal{F}_2\right) f^\dagger_{-1} \end{pmatrix}.$$

Here the $\mathcal{F}$ functions depend only on the $SO(5)$ constants Q and γ. $\mathcal{F}_0$ provides the coupling with the S states with seniority $(3\nu, 0)$, $\mathcal{F}_1$ takes care of coupling with the D states with seniority $(3\nu{+}1, 0)$, and $\mathcal{F}_2$ runs over the D states with seniority $(3\nu{+}2, 0)$.

References

[1] A. Ceulemans: *The theory of the Jahn-Teller effect* (Springer Nature Switzerland, 2022)

[2] A.F. Wells: *Structural inorganic chemistry* (Clarendon Press, Oxford, 1945)

[3] I.B. Bersuker: *The Jahn-Teller effect* (Cambridge University Press, 2006)

[4] J.T. Muya, J.D. Kelling, A. Ceulemans, C. Parish, J. Chem. Phys. **154**, 164305 (2021)

[5] F. Cocchini, T.H. Upton, J. Chem. Phys. **88**, 6068 (1988)

[6] T. Weike, D.M.G. Williams, A. Viel, W. Eisfeld, J. Chem. Phys. **151**, 074302 (2019)

[7] M.V. Berry: *The quantum phase, five years after* in: A. Shapere and F. Wilczek (eds.): *Geometric Phases in Physics*, Advanced Series in Mathematical Physics, Vol. 5, p. 7 (World Scientific, Singapore, 1989)

[8] M.T. Johnsson, G.E. Stedman, J. Phys.: Condens. Matter **11**, 787 (1999)

[9] A. Schilder, W. Bietsch, M. Schwoerer, New J. Phys. **1**, 5 (1999)

[10] B.R. Judd: *The theory of the Jahn-Teller effect* in C.D. Flint (ed.): *Vibronic processes in inorganic chemistry*, NATO ASI Series C: Mathematical and Physical Sciences, vol. 288, pp. 79-101 (Kluwer, Dordrecht, 1989)

[11] A. Auerbach, N. Manini, E. Tossatti, Phys. Rev. B **49**, 12998 (1994)